Available online at www.sciencedirect.com

ScienceDirect

journal homepage: www.elsevier.com/locate/he

Modeling the galvanic corrosion behavior of Pd–Cu couple used in hydrogen purification – PEM fuel cell hybrid systems

Farqad F. Al-Hadeethi [a,*], Hatem M. Alsyouri [b,c], Sohaib A. Dwairi [d]

[a] Scientific Research Center, Applied Science Sector, Royal Scientific Society, Amman, Jordan
[b] Department of Chemical Engineering, School of Engineering, The University of Jordan, Amman, Jordan
[c] Department of Chemical Engineering, College of Engineering and Technology, American University of the Middle East, Egaila, Kuwait
[d] Water and Environment Center, Applied Science Sector, Royal Scientific Society, Amman, Jordan

ARTICLE INFO

Article history:
Received 19 April 2016
Received in revised form
13 September 2016
Accepted 16 September 2016
Available online 14 October 2016

Keywords:
Galvanic corrosion
Pd/Cu couple
Modeling

ABSTRACT

Modeling the corrosion behavior of Pd/Cu couple in acidic media (0.25 M HCl) at various operating conditions [(30, 50 °C) and (0, 300, 600, 900 RPM)] was considered as an ultimate goal of this work. Multiple regression analysis with respect to ANOVA was utilized to generate a mathematical correlation. The derived correlation and the surface response revealed that increasing temperature and speed of agitation affected the corrosion rate of Cu in the Pd/Cu couple. This result indicates that using copper in the hydrogen purification – Proton Exchange Membrane (PEM) fuel cell hybrid systems is not acceptable due to the degradation that might occur as a direct result from the galvanic action between Pd/Cu couple. In order to improve the resistance of Pd against corrosion and hydrogen embrittlement at elevated temperatures, it should be alloyed with Au or Ag rather than copper.

Introduction

The use of hydrogen as an alternative source of energy is becoming increasingly addressed in research activities in terms of production, purification, storage and utilization in PEM fuel cells [1–4].

In these applications, the use of metals and alloys is unavoidable; for example, hydrogen produced by any suitable upstream process is purified using a hydrogen-selective metallic membrane made of Pd or Pd-based alloys. A wide range of variables have investigated and reported in literature. Basically, Nielsen et al. [5] have studied the effect of temperature on the corrosion of Cu–Pd hydrogen separation membrane alloys in simulated syngas containing H_2S. Medrano et al. [6] investigated Pd-based metallic supported membranes in fluidized bed reactor at high temperature, while Ghasemzadeh et al. [7] have evaluated the performance of dense Pd–Ag membrane reactor during methanol steam reforming using CFD analysis. Chen et al. [8] investigated the hydrogen permeation measurements of Pd and Pd–Cu membranes using dynamic pressure difference method. Decauxa et al. [9] have studied the time and frequency domain analysis of hydrogen permeation across Pd–Cu metallic membranes. Westerwaala et al. [10] investigated the hydrogen permeability of Pd–Cu based thin film membranes in relation to their structure. Achaa et al. [11,12] have studied the Pd–Cu

* *Corresponding author*. Fax: +962 65344806.
E-mail address: farqad.hadeethi@rss.jo (F.F. Al-Hadeethi).
http://dx.doi.org/10.1016/j.ijhydene.2016.09.123

membrane integration and lifetime in the production of hydrogen from methane as well as the copper deposition on Pd membranes by electroless plating.

Hydrogen is known to cause hydrogen embrittlement and to induce cracks in various kinds of metals including Pd. The risk of cracking becomes more aggressive when employing alloys such as Pd–Cu due to the anticipated galvanic corrosion between the couple. Galvanic (or dissimilar metal) corrosion can be defined as the corrosion that occurs as a result of one metal being in electrical contact with another in a conducting corrosive environment. The driving force for current and corrosion is the potential developed between the two metals. The more active metal (the anode) will be forced to be destructed, while the more noble metal (the cathode) will be fully or partially protected as mentioned by Schweitzer [13], Revie et al. [14], Hack [15], Saeed et al. [16]. However, the cathode may suffer from hydrogen damage when galvanic corrosion is taking place on the cathode. Galvanic corrosion is affected by several parameters including electrode specifications (type, exposed area, distance among electrodes, and geometry), electrolyte properties (acidity and purity), and other factors (temperature and motion) as mentioned by Hack [15], Saeed et al. [16] and Abdelhadi et al. [17].

To the best of our knowledge, galvanic corrosion has been rarely addressed in hydrogen-purifying metallic membranes. Such a study will be essential to develop alloys and setup strategies to confront galvanic corrosion to reduce the expenses, conserve materials, and above of all to improve safety as indicated by Basile et al. [18] and Yun et al. [19]. The purpose of this paper is to investigate galvanic corrosion of Pd–Cu couple under accelerated conditions using acidic medium (0.25 N HCl) at various operating temperatures (30 and 50 °C) and speeds of agitation (0, 300, 600, and 900 RPM), to simulate the galvanic corrosion behavior of real Pd–Cu in membranes. Results will be correlated and mapped using 3D facilities in order to verify the galvanic corrosion phenomenon and to improve the performance of the Pd based alloy membranes utilized in hydrogen purification – PEM fuel cell hybrid systems.

Experimental work

Materials

Specimens of copper (Nilaco Corporation, 99.93% purity), and palladium (Good fellow Cambridge Limited, 99.97% purity) were used. Palladium specimen with exposed surface area of 30 × 10 mm were utilized for the galvanic and single metal corrosion tests. On the other hand, for copper, 30 × 10 mm and 30 × 15 mm specimen were respectively used for galvanic corrosion and single metal corrosion tests.

Tests

Corrosion tests were performed using two devices: Potentiostat, and new-patented device called "Galvanic corrosion monitoring and analyzing system (GCMAS)". Potentiostat, was used to run potentiodynamic corrosion tests for single metallic specimens by generating the polarization curves (potential versus log (current density)) of Pd or Cu. Tested specimens (called Working Electrode, WE) were connected to the Reference Electrode, RE (Ag/AgCl – 3 M KCl) in order to measure the potential of the WE during the experiments. The WE is connected to an auxiliary electrode (called Counter Electrode, CE), to complete the electrical circuit. Fig. 1 shows the positions of WE, RE and CE within the corrosion cell.

Galvanic corrosion behavior of the Pd/Cu couple was tested using GCMAS as shown in Fig. 2. This device was developed and patented by the corresponding author [20–24]. It allows monitoring values and directions of the galvanic currents generated on both metals (Pd and Cu) with their coupling potential throughout the whole experiment. In order to operate GCMAS, flat metallic specimens made of different metals or alloys are coupled using the designed interface and kept at the bottom of the galvanic corrosion cell. The corrosive electrolyte is kept perpendicular to the specimens to allow the occurrence of electrochemical reactions on their surfaces.

Potentiodynamic polarization tests for single metallic specimens

Before conducting accelerated corrosion tests, Open Circuit Potential (OCP) of copper and palladium were determined by measuring the potential difference between the Working Electrode (WE) and Reference Electrode (RE) in the given electrolyte at the proposed temperatures (30 and 50 °C) for 30 min. The tested specimen (WE) is fixed inside the corrosion cell and connected to the reference and counter electrodes using electrical connectors. The electrolyte is poured inside the cell and set at the desired temperature and mixing rate using a hot plate. It is well known that potentiodynamic tests generate polarization curves at the tested operating conditions. Corrosion potential and current of each metal were determined using the intersection of Tafel slopes. Corrosion rates were calculated using the software package based on Equation (1).

$$C.R. = 0.00327 \times \frac{A \times i}{n \times \rho} \quad (1)$$

where: C.R.: corrosion rate (mm/y), A: atomic weight (g/mol), i: current density ($\mu A/cm^2$), n: number of electrons, and ρ: density of metal (g/cm^3). The constant 0.00327 is a conversion factor from $mAmp./cm^2$ to mm/y.

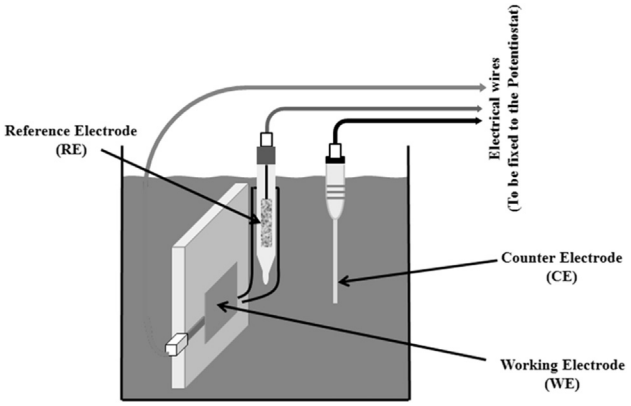

Fig. 1 – Schematic diagram shows the corrosion cell used during potentiodynamic tests.

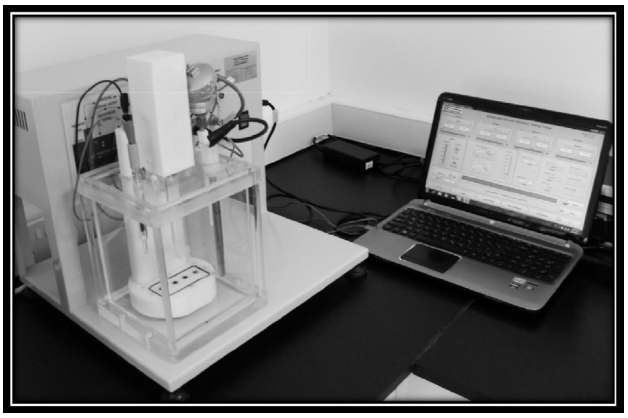

Fig. 2 – Galvanic corrosion monitoring and analyzing system (GCMAS).

Galvanic corrosion tests for coupled metallic specimens

Palladium and copper specimens were fixed to a special holder inside (GCMAS) in addition to the Reference Electrode (RE). Then the corrosive electrolyte is poured inside the cell at the desired temperature. Moreover, (GCMAS) control panel was used to measure and map galvanic currents and coupling potentials of the coupled metals without affecting the continuity of the electrochemical reactions. It was used also to measure and control the temperature and speed of agitation for the given electrolyte.

Hydrogen purification – PEM fuel cell hybrid system

Hydrogen Purification Unit (HPU, shown in Fig. 3 (a)) was connected to the PEM fuel cell system unit (shown in Fig. 3 (b)) to verify the performance of Pd–Cu membrane. It should be noted that HPU consists of an upstream gas delivery section, the cell, and a down-stream gas analysis section.

Results and discussion

Effect of temperature and speed of agitation on galvanic corrosion of Pd/Cu

Fig. 4 represents a key to understand Figs. 5 and 6 which show that the curves of the potentiodynamic polarization of Pd and Cu with their coupling potential versus time at the studied operating temperatures (30 and 50 °C) and speeds of agitation (0, 300, 600 and 900 RPM). The mentioned Figs. 5 and 6 indicated that Cu was aggressively corroded in order to protect Pd in the galvanic couple because the location of coupling potentials were below the polarization curves of Pd at the mentioned operating conditions as well as the polarization curve of Cu indicates clearly higher corrosion current densities than Pd based on the intersection value of the cathodic portion with the anodic portion of Tafel region within each polarization curve without forgetting the effect of increasing the speed of agitation (0, 300, 600 and 900 RPM) which played a crucial role in changing the corrosion rates in both Cu and Pd. On the other hand, Table 1 shows the average galvanic currents ($I_{g,av}$) of Cu which represents the rate of galvanic corrosion of the active part in the Pd/Cu couple obtained by calculating the area under the curve using trapezoidal rule of the curves generated using GCMAS System as shown in Figs. 7 and 8 which represents the curves of the galvanic currents of Pd/Cu couple (Ig_{pd} and Ig_{cu}) vs. time and the coupling potential ($E_{coupling}$) vs. time at the selected operating conditions. The results revealed that the average galvanic currents ($I_{g,av}$) of Cu increase with increasing the speed of agitation from 0 to 900 RPM at both temperatures (30 and 50 °C). Whereas, the average galvanic currents ($I_{g,av}$) of Cu decreased with increasing temperature at all speeds of agitation except at 900 RPM.

In other words, the extracted results were in agreement with Schweitzer [13], Revie et al. [14], Hack [15], Saeed et al. [16]. Taking into consideration that the results of galvanic

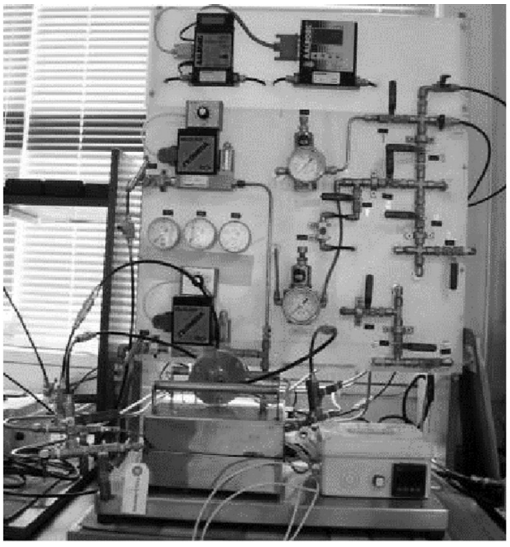

(a)

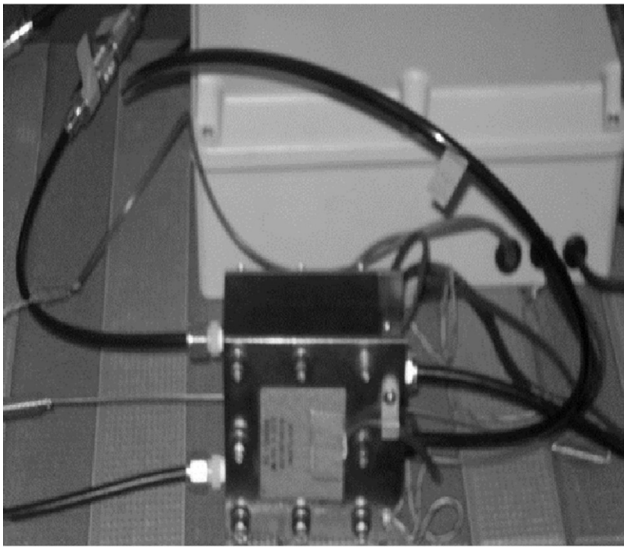

(b)

Fig. 3 – (a) Hydrogen purification unit (HPU). (b) PEM fuel cell unit.

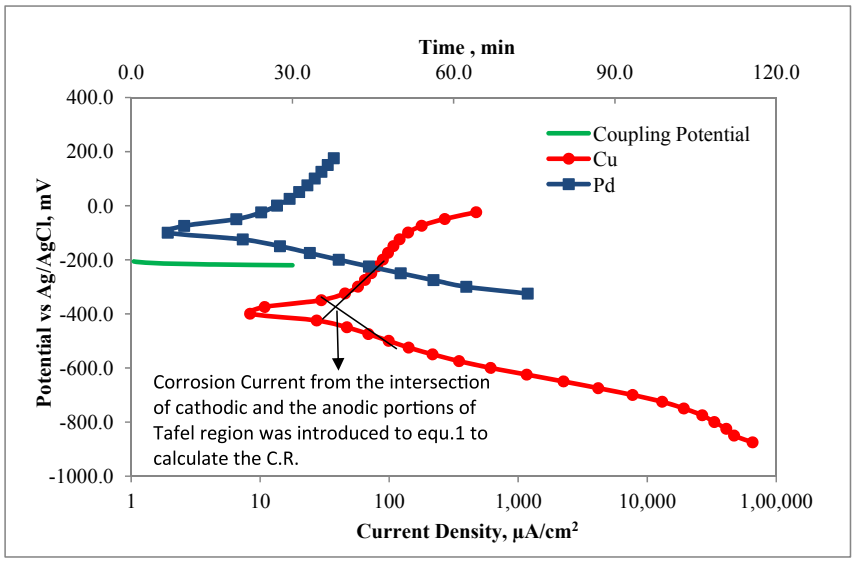

Fig. 4 – Typical potentiodynamic polarization curves of palladium and copper along with their coupling potential. This is a key to understand the details of Fig. 5 and 6 where the coupling potential was obtained from GCMAS while the polarization curves of Cu and Pd were obtained from the potentiodynamic test.

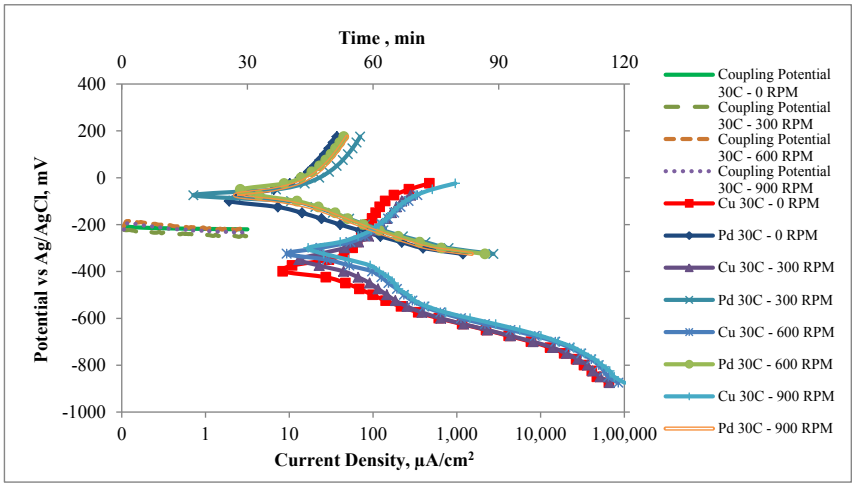

Fig. 5 – Potentiodynamic polarization curves of palladium and copper with their coupling potential in 0.25 M HCl at 30 °C and different speeds of agitation.

corrosion between Pd and Cu was affected by several parameters (i.e. type, exposed area, distance between electrodes, and geometry), electrolyte properties (acidity and purity), in addition to (temperature and speed of agitation) and this is in agreement with Abdelhadi et al. [17] and Saeed et al. [25].

Generating the mathematical correlation

Equation (2) was generated using multiple regression analysis with respect to ANOVA provided by MATLAB software package, where ANOVA is used to determine how well the generated mathematical correlation explains the response variable [35]. The resulting ANOVA Tables 2 and 3 for Equation (2) outline the analysis of variance for each response including R^2 and *Adjusted* R^2, which indicates the significance of the generated mathematical correlation since *Adjusted* R^2 is greater than the acceptable value of 85%, F value (i.e. the ratio of the treatment variance to the error variance) is highly greater than F critical, and p-value (i.e. the observed significance level) is less than the preset α of 0.05 (i.e. the critical level of significance), taking into consideration that t-test values could be compared with t-critical values and used as the hypothesis test criterion instead of p-values at the given degrees of freedom and α [36]. The entire adequacy measures are in agreement with the general outlines provided by Eltawahni et al. [26,27].

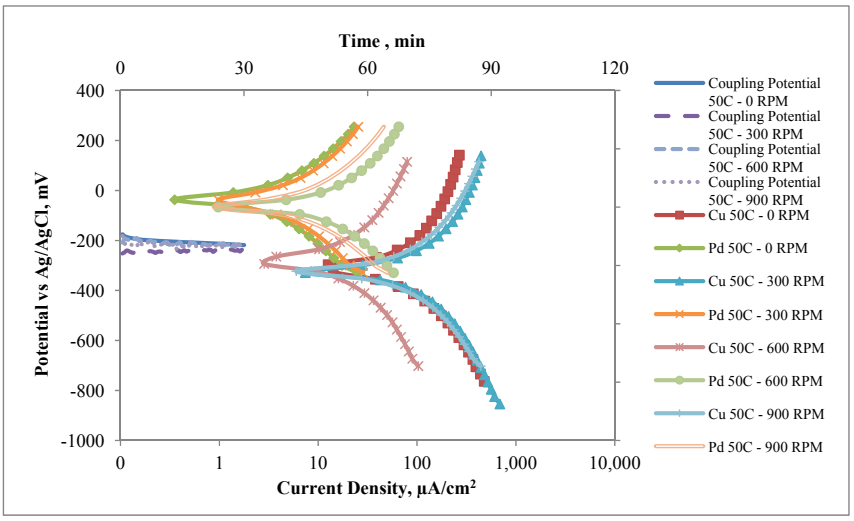

Fig. 6 – Potentiodynamic polarization curves of palladium and copper with their coupling potential in 0.25 M HCl at 50 °C and different speeds of agitation.

On the other hand, Tables 4 and 5 show a comparison between the actual values of the average galvanic currents of Pd/Cu couple ($I_{g,\ av}$) as a function of temperature (T) and speed of agitation (S) obtained through GCMAS during the experiments and the values of ($I_{g,\ av}$) predicted using Equation (2). In fact, Tables 4 and 5 indicate that the predicted values are very close to the actual values. All the above measures assured the significance of Equation (2). A new temperature was introduced in Table 5 [i.e. 40 °C] and new values for $I_{g,av}$ were generated which assured the significance of the generated mathematical correlation in Equation (2).

$$I_{g,av} = 6863.539 - 91.4679 \times T + 0.00186 \times T^2 \times S \quad (2)$$

where:

$I_{g,av}$: average galvanic current in (µAmp.).
T: temperature in (°C)
S: speed of agitation in (RPM)

Three dimensional mapping (i.e. shaded surface plot which is called surface response) of Equation (2) was represented in Fig. 9. The surface response given in Fig. 9 clearly shows the interaction among the independent variables [temperature (T) and speed of agitation (S)] and the average galvanic currents of

Table 1 – Average galvanic currents of Cu ($I_{g,av}$) in Pd/Cu couple immersed in 0.25 M HCl at different conditions.

Agitation speed (rpm)	Temperature	
	30 °C	50 °C
0	3505[a]	2576[a]
300	4899[a]	3761[a]
600	5339[a]	4457[a]
900	5748[a]	6736[a]

[a] $I_{g,\ av}$. (µAmp.).

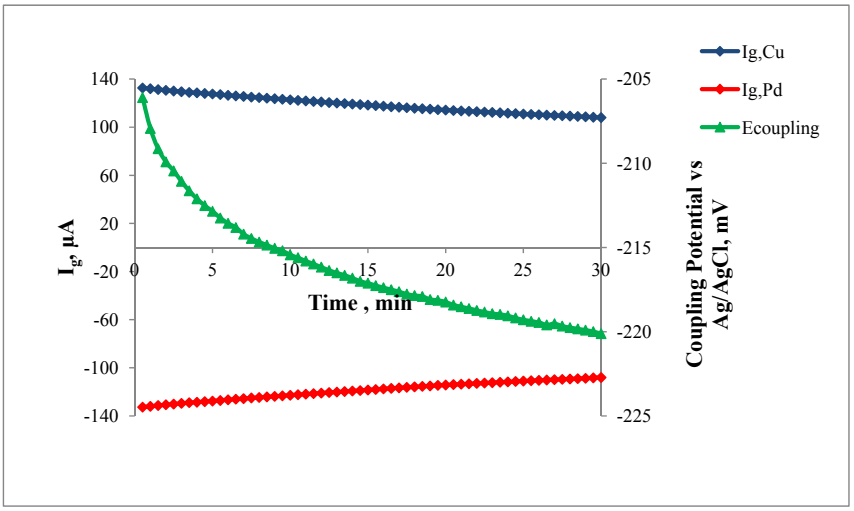

Fig. 7 – Galvanic currents of Pd and Cu with their coupling potential in 0.25 M HCl at 30 °C, 0 RPM.

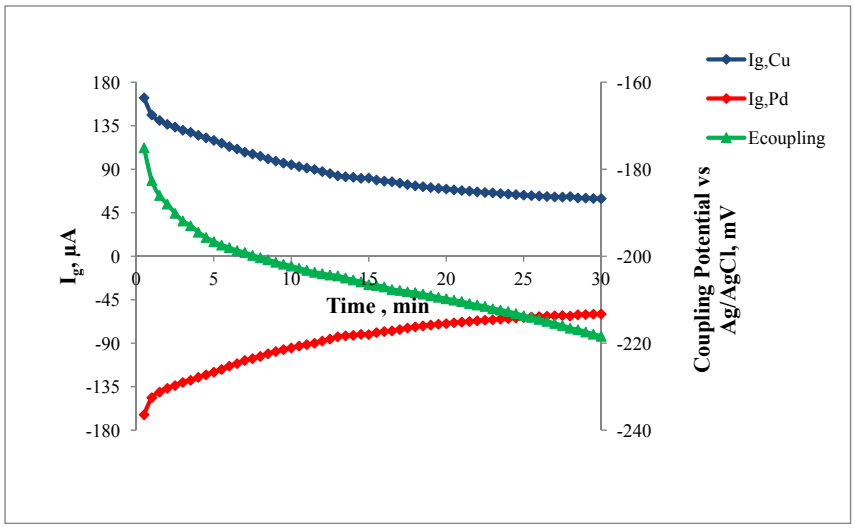

Fig. 8 – Galvanic currents of Pd and Cu with their coupling potential in 0.25 M HCl at 50 °C, 0 RPM.

Table 2 – Analysis of variance for the correlation in Equation 2.

Source of variation	Sum of squares (SS)	Degrees of freedom (df)	Mean square (MS)	F	F critical
Regression	0.03×10^8	2	51,555,938	87.51621	3.4668
Residual	12,371,133	21	589101.6		
Total	1.15×10^8	23			
R-square (%)	91.5				
Adjusted R-square (%)	88.2				

Table 3 – Analysis of the coefficients for each regressor in Equation 2.

	Coefficient	Standard error (SE)	T test	P
Intercept	6863.539	693.2939	9.899898	0.000179
T	−91.4679	18.74302	−4.8801	0.004553
$T^2 \times S$	0.00186	0.000258	7.201708	0.000804

Pd/Cu couple ($I_{g,\,av}$) which confirms the explanations given in Section Effect of temperature and speed of agitation on galvanic corrosion of Pd/Cu. Fig. 9 assures the general trend of corrosion rate of Pd/Cu obtained during the experiments.

According to Table 4, errors in the predicted average galvanic current value under studied conditions are in the range of 2–17.5%. As a result, it is obvious that the galvanic coupling of Pd and Cu will have a negative impact on the performance when used as a membrane for hydrogen purification. The corrosion action on Cu will cause the membrane to deteriorate quickly. Besides, palladium membranes already become brittle and lose their ductility in the presence of hydrogen. It is worth to mention that pure palladium membranes used for hydrogen purification suffer also from poisoning problem as well as thermal and mechanical stability challenges as indicated by a number of research investigations [28–33].

Alloying Pd with other metals such as copper will decrease the cost of this kind of membrane [5], however, alloying will be accompanied by a simultaneous galvanic corrosion, resulting in the generation of defects and pinholes within structure of the membrane. In order to improve the resistance of Pd against corrosion and hydrogen embrittlement at

Table 4 – Actual and predicted values of the average galvanic currents of Pd/Cu couple at the studied operating conditions, with the percent difference between them.

Temperature (T), °C	Speed of agitation (S), RPM	Actual average galvanic current ($I_{g,\,av}$), µA	Predicted average galvanic current ($I_{g,\,av}$), µA using Equation (2)	% Difference
30	0	3505	4120	17.5
	300	4899	4622	−5.7
	600	5339	5124	−4.0
	900	5748	5626	−2.1
50	0	2576	2290	−11.1
	300	3761	3685	−2.0
	600	4457	5080	14.0
	900	6736	6475	−3.9

Table 5 – Average galvanic currents ($I_{g,\ av}$) of Pd/Cu couple in 0.25 M HCl at selected temperatures and speeds of agitation; actual values and predicted by the mathematical correlation.

Speed of agitation (S), RPM	Actual average galvanic current ($I_{g,\ av}$), μA		Predicted average galvanic current ($I_{g,\ av}$), μA using Equation (2)		
	30 °C	50 °C	30 °C	40 °C	50 °C
0	3505	2576	4120	3205	2290
200	–	–	4454	3800	3220
300	4899	3761	4622	4098	3685
500	–	–	4956	4693	4615
600	5339	4457	5124	4990	5080
700	–	–	5291	5288	5545
900	5748	6736	5626	5883	6475

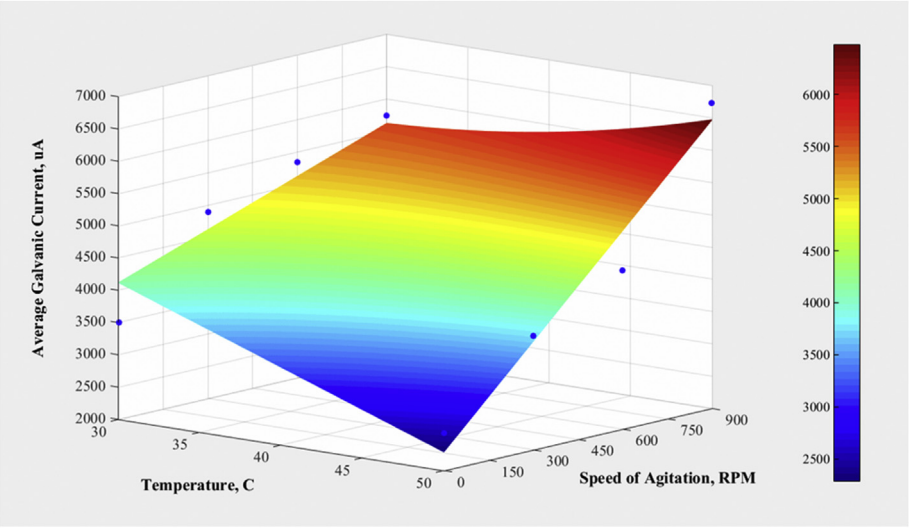

Fig. 9 – Surface response of Equation (2).

elevated temperatures, it should be alloyed with Au or Ag because their potentials are very near to Pd in the galvanic series. Copper which is considered more anodic to Pd in the galvanic series, so alloying Pd with Cu causes it to corrode rapidly as a direct result of galvanic corrosion generated between Pd/Cu. This opinion is in agreement with Lewis et al. [34].

Conclusions

The results revealed that increasing temperature and/or speed of agitation will affect the corrosion rate of Pd/Cu couple. The derived correlation for Pd/Cu and three dimensional mapping (i.e. surface response) showed clearly the interactions among different variables (temperature and speed of agitation) on the corrosion rate of coupled metals (Pd/Cu). This result indicates that using copper in hydrogen purifiers is not acceptable due to the degradation that occurs as a direct result from the galvanic action between Pd/Cu. In order to improve the corrosion resistance of Pd against corrosion and hydrogen embrittlement at elevated temperatures corrosion, it should be alloyed with Au or Ag rather than copper which is considered more anodic to Pd in the galvanic series.

Acknowledgements

The authors would like to thank the Corrosion and Electrochemical Reaction Engineering Lab./Scientific Research Center/Applied Science Sector/Royal Scientific Society for sponsoring and hosting all research activities of the present work. The authors would like also to thank Eng.Amani Abdelhadi (M.Sc.)/senior research assistant for her efforts during the experimental part of the present work.

REFERENCES

[1] Iranzo A, Boillat P, Biesdorf J, Salva A. Investigation of the liquid water distributions in a 50 cm^2 PEM fuel cell: effects of reactants relative humidity, current density, and cathode stoichiometry. Energy J 2015;82:914–21.

[2] Amica G, Arneodo Larochette P, Gennari FC. Hydrogen storage properties of LiNH2eLiH system with MgH_2, CaH_2 and TiH_2 added. Int J Hydrogen Energy 2015;40:9335–46.

[3] Saeed F, Saidan M, Said A, Mustafa M, Abdelhadi A, Al-Weissi S. Effect of flow rate, flow direction, and silica addition on the performance of membrane and the corrosion

behavior of Pt–Ru/C catalyst in PEMFC. Energy Convers Manag 2013;75:36–43.
[4] Saeed F, Alsyouri H, Al-Ghandoor A, Al-Husban Y, Abdelhadi A, Al-Weissi S. Developing an integrated solar powered system to generate hydrogen from sea water. Int J Electrochem Sci 2013;8:6311–20.
[5] Nielsen B, Dogan O, Howard B. Effect of temperature on the corrosion of Cu-Pd hydrogen separation membrane alloys in simulated syngas containing H_2S. Int J Corros Sci 2015;96:74–86.
[6] Medrano J, Fernandez E, Melendez J, Parco M, Tanaka D, Annaland M, et al. Pd-based metallic supported membranes: high-temperature stability and fluidized bed reactor testing. Int J Hydrogen Energy 2016;41:8706–18.
[7] Ghasemzadeh K, Andalib E, Basile A. Evaluation of dense Pd–Ag membrane reactor performance during methanol steam reforming in comparison with autothermal reforming using CFD analysis. Int J Hydrogen Energy 2016;41:8745–54.
[8] Chen W, Hsu P. Hydrogen permeation measurements of Pd and Pd–Cu membranes using dynamic pressure difference method. Int J Hydrogen Energy 2011;36:9355–66.
[9] Decauxa C, Ngamenic R, Solasc D, Grigorievd S, Milletc P. Time and frequency domain analysis of hydrogen permeation across Pd-Cu metallic membranes for hydrogen purification. Int J Hydrogen Energy 2010;35:4883–92.
[10] Westerwaala R, Boumand E, Haijea W, Schreudersa H, Duttaa S, Wub M, et al. The hydrogen permeability of Pd–Cu based thin film membranes in relation to their structure: a combinatorial approach. Int J Hydrogen Energy 2015;40:3932–43.
[11] Achaa E, Requiesa J, Barrioa V, Cambraa J, Güemeza M, Ariasa P, et al. PdCu membrane integration and lifetime in the production of hydrogen from methane. Int J Hydrogen Energy 2013;38:7659–66.
[12] Achaa E, Delftb Y, Overbeekb J, Ariasa P, Cambraa J. Copper deposition on Pd membranes by electroless plating. Int J Hydrogen Energy 2011;36:13114–21.
[13] Schweitzer PA. Fundamentals of corrosion. 1st ed. New York: CRC Press; 2010.
[14] Revie RW, Uhlig HH. Corrosion and Corrosion Control. 3rd ed. New York: John Wiley and Sons; 2008.
[15] Hack H. Galvanic corrosion. Philadelphia: ASTM; 1988.
[16] Saeed F, Abdelhadi A, Abbasi G. Managing galvanic corrosion in industry. 1st ed. Germany: LAP; 2011.
[17] Abdelhadi A, Abbasi G, Saeed F. Estimating the life time of industrial mechanical structures facing metallic corrosion phenomena in acidic environment [M.S. thesis]. Jordan: University of Jordan; 2010.
[18] Basile A, Gallucci F. Membranes for membrane reactors: preparation, optimization and selection. John Wiley and Sons; 2011.
[19] Yun S, Oyama S. Correlations in palladium membranes for hydrogen separation: a review. J Membr Sci 2011;375:28–45.
[20] Saeed F. U.S. Patent US20080257729 A1, 2008.
[21] Saeed F. European Patent EP1956357, 2007.
[22] Saeed F. Japanese Patent JP20080025219 20080205, 2008.
[23] Saeed F. Indian Patent 246/DEL/2008, 2008.
[24] Saeed F. Jordanian Patent JO2377, 2006.
[25] Saeed F. Computer aided simulation and laboratory investigation of activation controlled galvanic corrosion [Published Doctoral Dissertation]. Iraq: Saddam University; 2001.
[26] Eltawahni HA, Hagino M, Benyounis KY, Inoue T, Olabi AG. Effect of CO2 laser cutting process parameters on edge quality and operating cost of AISI316L. Opt Laser Technol J 2012;44(4):1068–82.
[27] Eltawahni HA, Olabi AG, Benyounis KY. Effect of process parameters and optimization of CO2 laser cutting of ultra high-performance polyethylene. Mater Des J 2010;31(8):4029–38.
[28] Hu X, Huang Y, Shu S, Fan Y, Xu N. Toward effective membranes for hydrogen separation: multichannel composite palladium membranes. J Power Sources 2008;181:135–9.
[29] Lin YM, Rei MH. Separation of hydrogen from the gas mixture out of catalytic reformer by using supported palladium membrane. Sep Purif Technol 2001;25:87–95.
[30] Ryi SK, Park JS, Kim SH, Cho SH, Hwang KR, Kim DW, et al. A new membrane module design with disc geometry for the separation of hydrogen using Pd alloy membranes. J Membr Sci 2007;297:217–25.
[31] Chen W, Hsia M, Lin Y, Chi Y. Hydrogen permeation and recovery from $H_2 - N_2$ gas mixtures by Pd membranes with high permeance. Int J Hydrogen Energy 2013;38:14730–42.
[32] Zhang X, Wang W, Liu J, Sh Sheng, Xiong G, Yang W. Hydrogen transport through thin palladium-copper alloy composite membranes at low temperatures. Thin Solid Films 2007;516:1849–56.
[33] Nielsen BC, Doğan ON, Howard BH, Nall E. Comparison of the corrosion of Cu50Pd50 and Cu50Pd44M6 (M = Y, Mg, or Al) hydrogen separation membrane alloys in simulated syngas containing H_2S. Corros Sci 2013;76:170–81.
[34] Lewis AE, Zhao H, Syed H, Wolden CA, Way JD. PdAu and PdAuAg composite membranes for hydrogen separation from synthetic water-gas shift streams containing hydrogen sulfide. J Membr Sci 2014;465:167–76.
[35] Jongman RHG, Ter Braak CJF, Van Tongeren OFR. Data analysis in community and landscape ecology. Cambridge University Press; 1995.
[36] Ken B. Business statistics for contemporary decision making. 6th ed. John Wiley and Sons, Inc.; 2010.